Spin-imbalances in non-magnetic nano-systems: Using non-equilibrium Green's function DFT to model spin-selective phenomena mediated by spin-orbit coupling.

W. Dednam[1,2], Linda A. Zotti[3], S. Pakdel[4], E. B. Lombardi[1] and J. J. Palacios[5]

[1] Department of Physics, Science Campus, University of South Africa, Private Bag X6, Florida Park 1710, South Africa
[2] Departamento de Física Aplicada and Unidad Asociada CSIC, Universidad de Alicante, Campus de San Vicente del Raspeig, E-03690 Alicante, Spain.
[3] Departamento de Física Teórica de la materia condensada, Universidad Autonoma de Madrid, Cantoblanco, Madrid 28049, Spain
[3] Department of Physics, Technical University of Denmark: Kongens Lyngby, Hovedstaden, Denmark
[4] Departamento de Física de la Materia Condensada, Universidad Autonoma de Madrid, Cantoblanco, Madrid 28049, Spain

E-mail: dednaw@unisa.ac.za

Abstract. Heavy transition metals are frequently used as electrodes and substrates in scanning tunneling microscopy experiments. In the constricted low dimensional systems that occur in such experiments, typically under conditions of non-zero bias voltage, spin-imbalance may develop even in non-magnetic atomic- and nano-systems. This phenomenon arises as a result of spin selective effects mediated by spin-orbit coupling. It is important to not only understand the emergence of the spin imbalance, but also to model associated properties such as spin-polarized electron transport in these systems. Conventional theoretical approaches cannot model these effects because they usually neglect spin-orbit coupling. Therefore, to model spin-imbalance in the electronic transport of constricted nano-systems, such as in atomically sharp transition metal electrode tips or surfaces, as well as in organic molecules bridging the electrode tips, we have implemented spin-orbit coupling as a post-self-consistent correction in atomic orbital basis density functional theory within the non-equilibrium Green's function formalism. Our method takes advantage of optimized Gaussian orbital basis sets and effective core potentials and one-shot transport calculations with steady convergence and charge transfer properties compared to other similar approaches. We apply this method to a selected number of sample constricted low dimensional systems where spin-imbalance is important by performing density functional transport calculations. This permits us to demonstrate that incorporation of spin-orbit coupling is essential to understanding emergent spin-imbalance in molecular electronics, while in certain instances, the consideration of the applied bias is also important to the manifestation of spin imbalance phenomena in heavy transition metal electrodes and substrates.

1. Introduction

Spintronics is a promising field in which the electron's spin is used to process and store information as an improvement on the present use of its charge to accomplish those same tasks [1]. Recently, spin-orbit coupling (SOC) has been proposed as an explanation for spin-polarized currents in molecular junctions [2, 3, 4, 5], which, in the simplest possible arrangement, consist of two nano-sized transition metal electrodes bridged by freely-suspended chiral organic molecules (molecules which have non-superimposable mirror images), typically in the scanning tunneling microscope (STM) setup [6, 7]. In practical applications, spin-selective molecular nano-junctions could serve, for example, as spin-current rectifiers in novel spintronic molecular devices, due to the so-called chirality induced spin selectivity (CISS) effect.

There still exists, however, a controversy surrounding the exact origin of the CISS effect: is it due to spin-locking along the twisting chiral molecule in which orbit moments on the molecule's atoms favour the transport of one spin orientation over another [2], or does the molecule inherit SOC from the heavy transition metal electrodes such that spin-filtering rather take places at the interface between metal electrode and molecule [3, 4, 5]? To answer this question from a theoretical perspective, it is at the very least necessary to model SOC properly and conveniently in electronic transport calculations based on density functional theory (DFT), since comparisons with experiment are usually accomplished via such calculations [7, 8, 9]. SOC transport calculations are possible in many DFT codes, but convergence may be intractable for nano-systems involving more than a few tens of (heavy transition metal) atoms. In this work, we present one-shot DFT electronic transport calculations based on the non-equilibrum Green's function (NEGF) method [8] using Gaussian-type orbital(GTO) basis sets that have been fitted to high quality SOC bands.

2. Models

In 2018, Pakdel et al. [10] found that if a GTO basis set describes the band structure of a material well in the absence of SOC, then adding SOC as a correction in a post self-consistent-field (SCF) step gives good SOC bands, when compared to a reference method that produces very high quality bands such as `VASP` [11], `Wien2k` [12], `Quantum Espresso` [13] or `OpenMX` [14, 15, 16, 17]. Pakdel et al.'s method [10] and our recent improvements thereupon are described very briefly below.

The Dirac-Kohn-Sham Hamiltonian can be written, to lowest order, as the standard atomic SOC matrix because the radial and angular components of the wave functions in atomic-orbital based DFT, such as the GTOs used by `CRYSTAL14` [18] or `GAUSSIAN09` [19] are orthogonal:

$$\xi\left(r\right)\mathbf{L}\cdot\mathbf{S}=\left[\xi_{\mathrm{ij}}\left\langle l_{\mathrm{i}};m_{l_{\mathrm{i}}};s|\mathbf{L}\cdot\mathbf{S}|l_{\mathrm{j}};m_{l_{\mathrm{j}}};s'\right\rangle\right], \tag{1}$$

where:

$$\xi_{\mathrm{ij}}=\frac{e^2}{2m_ec^2}\int_0^\infty\frac{1}{r}\frac{\mathrm{d}V_{\mathrm{eff}}\left(r\right)}{\mathrm{d}r}R_{\mathrm{i}}\left(r\right)R_{\mathrm{j}}^*\left(r\right)r^2\mathrm{d}r. \tag{2}$$

In equation (2), $V_{\mathrm{eff}}\left(r\right)=-\frac{Z}{r}$ is the effective nuclear potential [10], with Z the atomic number. $R_{\mathrm{i}}\left(r\right)$ are the radial (un)contracted gaussian-type orbitals (CGTOs). Only CGTOs on the same atom and of the same shell type ($L=1$, 2 or 3) contribute to the integral because SOC is an intra-atomic phenomenon [10]. However, for CGTO basis sets with pseudopotentials, Pakdel et al. found that a single multiplicative correction to ξ_{ij} was needed in order to account for the correct effective charge in $V_{\mathrm{eff}}\left(r\right)$ due to the lack of nodal structure near the nucleus in pseudopotentials. Here, we make two minor modifications to improve the above implementation. We use the following modified Yukawa screening potential:

$$V_{\mathrm{eff}}\left(r\right)=\begin{cases}\frac{-(Z-1)\left[\exp\left(-\frac{lnZ}{r_c}r\right)+1\right]}{r} & r\leq r_c\\ \frac{-1}{r} & r>r_c\end{cases} \tag{3}$$

where r_c is a cutoff, typically the size of an atomic radius ($\sim 2.5-3.0$ a.u.). Instead of the single global multiplicative factor used in ref. [10], we implement a multiplicative factor for each shell type ($L = 1$, 2 or 3) to account for the fact that the radial SOC coefficients of different shells are usually multiples of each other [20].

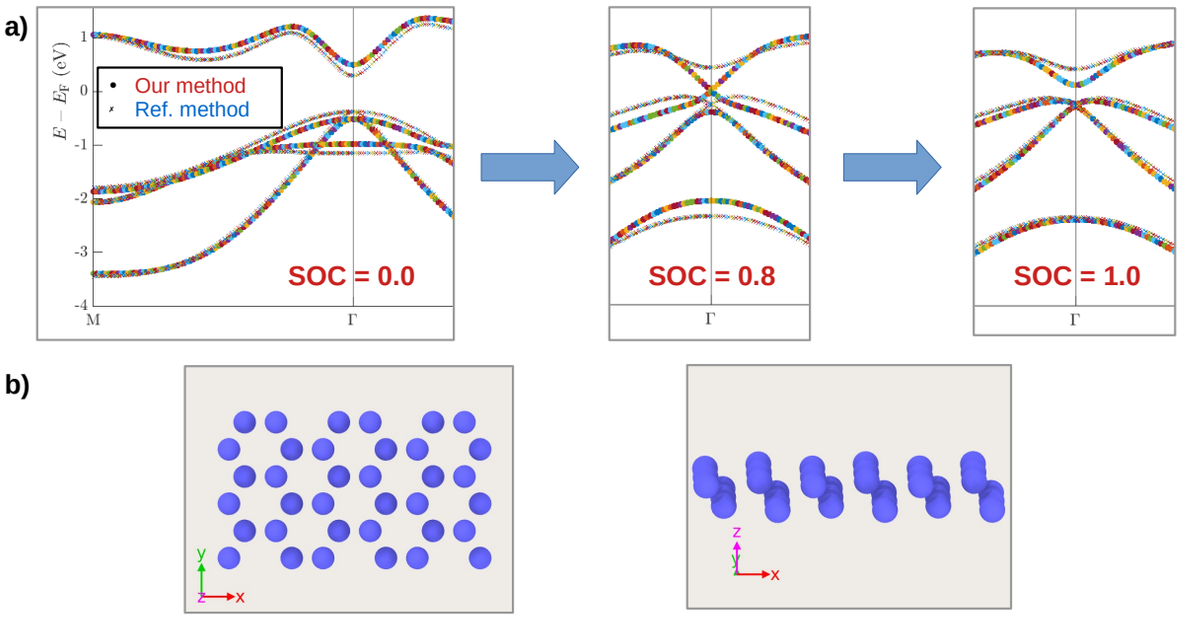

Figure 1. (Colour online) a) Example of adding spin-orbit coupling as a post-SCF correction in DFT calculations of the bands of a solid material, for b) Bismuth (111) bilayers. Solid markers are our method and the fainter crosses correspond to the reference method. The same lattice parameters were used in both methods as in ref. [10]: $a = 4.33$ Å and $c = 1.74$ Å in symmetry group $P\bar{3}m1$ of the Hermann-Mauguin classification or space group 164 in the International Tables of Crystallography.

3. Results and discussion

To verify that adding SOC as a correction in a post-SCF step gives good SOC bands, we use Bi(111) bilayers (see figure 1 b)) as a test system and compare our calculations using `CRYSTAL14` on one hand, and `OpenMX` as reference method, on the other, given the very good agreement between `OpenMX` and `Wien2k` [21, 22].

In Bi(111) bilayers, starting without SOC in the left panel of figure 1 a), the band gap must evolve first into a Dirac cone at the Γ point (SOC=0.8 in the middle panel of figure 1 a)) and then open up again as SOC is increased to 1.0 in a so-called "band inversion" in the rightmost panel of figure 1 a). We used the high quality basis set from ref. [23] for Bi and the Perdew-Burke-Ernzerhof (PBE) generalized-gradient approximation (GGA) exchange correlation functional in our `CRYSTAL14` calculation of the bands in the absence of SOC, resulting in reasonable agreement with our reference method, using the `Bi8.0-s4p4d3f2` basis set and `Bi_PBE19` pseudopotential in `OpenMX`. We also used very large k meshes ($81 \times 47 \times 1$) in multiples of 3 to correctly capture the electronic structure at the Γ point. In going from SOC=0.0 to SOC=1.0, we only tuned the multiplicative factor empirically for the bands of p-orbital ($L = 1$ shell) character because only

they contribute to SOC ±4 eV about the Fermi energy. Thus, in figure 1, SOC=0.8 corresponds to using a $L = 1$ multiplicative factor SOCFAC$_P$ = 270.0 and SOC=1.0, to SOCFAC$_P$ = 350.0.

The ultimate goal of fitting SOC corrected bands to a reference method is to choose high quality basis sets that can be used in DFT electronic transport calculations where transition metal elements, sometimes with strong SOC, are used as the electrodes. We therefore need high quality GTO basis sets for metals such Au, Ag and Cu, which are used in experiments [24, 25]. For the sake of brevity, we present only the SOC-corrected bands for two extreme cases (see figure 2): face-centred cubic (FCC) Cu using an all-electron basis set [26] (all multiplicative factors set equal to 1.0) and FCC Au using the high quality pseudopotential basis set reported in ref. [23]. The latter required larger per-shell multiplicative factors, SOCFAC$_P$ = 260.0, SOCFAC$_D$ = 40.0 and SOCFAC$_F$ = 10.0 for the $L = 1, 2, 3$ shells respectively. The same lattice parameters were used in our and the reference methods: 3.63 Å in the case of Cu and 4.05 Å for Au [23]. As basis sets and pseudopotentials in `OpenMX`, we used `Cu6.0H-s3p3d3f1` and `Cu_PBE19H` for Cu and `Au7.0-s2p2d2f1` and `Au_PBE19` for Au.

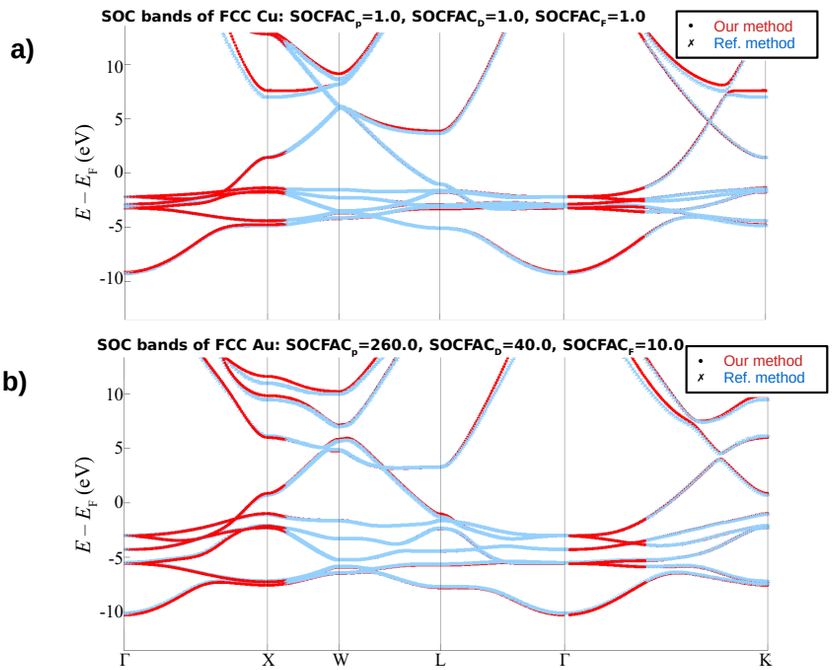

Figure 2. (Colour online) a) SOC-corrected bands for face-centred cubic Cu obtained using the all-electron basis set reported in ref. [26] in `CRYSTAL14` (red solid markers) and the reference method `OpenMX` (light blue crosses) b). SOC-corrected bands for FCC Au obtained using the pseudopotential basis set reported in ref. [23] in `CRYSTAL14` (red solid markers) and the reference method `OpenMX` (light blue crosses). Notice that per-shell multiplicative SOC factors much larger than 1 were needed to get a good empirical fit in the case of Au.

Figure 3 illustrates two simple example applications of our post-SCF electronic transport implementation of SOC. For this, we use the code Atomistic NanoTransport (`ANT.Gaussian`) [27, 28, 29]. It interfaces with `Gaussian09` [19] to perform a scalar-relativistic, spin-unrestricted calculation of the transport. The SOC correction has been implemented in `ANT.Gaussian` and is freely available online [30]. The advantage of using `ANT.Gaussian` over other density functional theory (DFT) codes with a self-consistent SOC electronic transport capability, is that the calculation requires just one step unlike most of the other codes in which a one-dimensional

ISBN: 978-0-620-97693-0
ISBN: 978-0-620-97693-0

electrode model is used [31, 32]. Moreover, our method displays better convergence properties compared to other codes in the absence of SOC, such as our reference method `OpenMX` [33, 32].

The structure in figure 3 a) was taken directly from the online supplementary material of ref. [4]. For Au and Cu, we used the basis sets referred to previously. For Ag, a pseudopotential basis set giving good agreement with the reference method and similar to that of Au was used [34]. As expected, the polarization in the molecule generally increases as the metal becomes heavier and the intra-atomic SOC interaction becomes larger.

In figure 3 b), we show the manifestation of the classical spin-Hall effect in an unreconstructed surface of Au(111). Broken inversion symmetry in thin samples or exposed surfaces of heavy transition elements leads to the lateral separation of spins of roughly opposite orientation under non-zero bias, 0.1 and 0.5 V, even in non-magnetic materials [35].

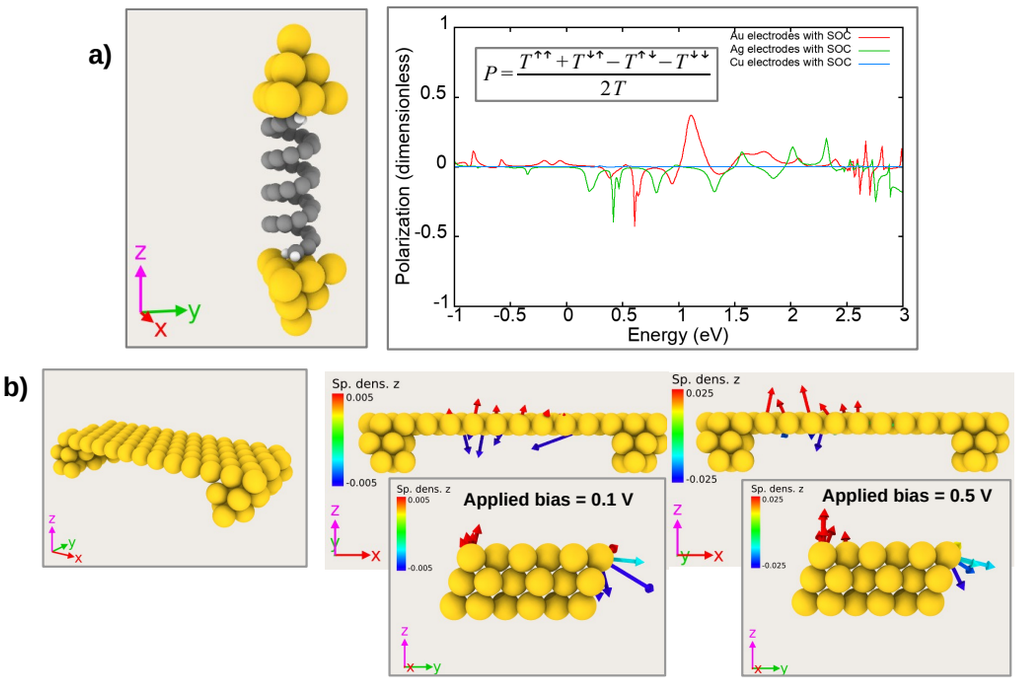

Figure 3. (Colour online) a) Polarization (P) of the helicene molecule sandwiched between Au, Ag or Cu electrodes (left) as a function of energy, calculated at zero bias voltage from the spin-resolved transmission $T^{\sigma,\sigma'}$, where $\sigma, \sigma' = \{\uparrow, \downarrow\}$. b). Spin densities along the z direction in the Au "table" shown on the left and calculated at bias voltages of 0.1 and 0.5 V, respectively. Under non-zero bias, the classical spin Hall effect manifests as the lateral separation, along the transport direction, of spins of approximately opposite orientation.

4. Conclusion

We have presented a post self-consistent field implementation of spin-orbit coupling in density functional theory calculations on transition metals using Gaussian type local orbitals. The ability of such basis sets to correctly reproduce the electronic structure of the metals is established by comparing spin-orbit-coupling corrected bands with those generated by a fully self-consistent implementation of the spin-orbit interaction. The transferrability of the basis sets to density functional theory electronic transport calculations was established by performing simple test calculations to reproduce phenomena that are known to trace their origins to spin-orbit coupling: (i) chirality induced spin selectivity of organic molecules under zero bias and

(ii) the manifestation, under non-zero bias, of the classical spin Hall effect in a thin non-magnetic Au(111) surface. The advantage of our method is that the calculation is one-shot, i.e., requires only one step and also exhibits superior convergence properties compared to other fully-relativistic self-consistent implementations. In future work, we will implement SOC-corrected band fitting for magnetic systems and composite materials.

Acknowledgments
The computational results contained in this work would also not have been possible without access to the high performance computing (HPC) facility at Unisa, and the supercomputing facility in the Department of Applied Physics at the University of Alicante.

References

[1] Joshi V K 2016 *Engineering Science and Technology, an International Journal* **19** 1503–1513
[2] Dalum S and Hedegård P 2019 *Nano Letters* **19** 5253–5259
[3] Zöllner M S, Varela S, Medina E, Mujica V and Herrmann C 2020 *Journal of Chemical Theory and Computation* **16** 2914–2929
[4] Zöllner M S, Saghatchi A, Mujica V and Herrmann C 2020 *Journal of Chemical Theory and Computation* **16** 7357–7371
[5] Liu Y, Xiao J, Koo J and Yan B 2021 *Nature Materials* **20** 638–644
[6] Binnig G, Rohrer H, Gerber C and Weibel E 1982 *Phys. Rev. Lett.* **49**(1) 57–61
[7] Agraït N, Yeyati A L and Van Ruitenbeek J M 2003 *Physics Reports* **377** 81
[8] Cuevas J C and Scheer E 2010 *Molecular Electronics* (Singapore: World Scientific)
[9] Requist R, Baruselli P P, Smogunov A, Fabrizio M, Modesti S and Tosatti E 2016 *Nat. Nanotechnol.* **11** 499
[10] Pakdel S, Pourfath M and Palacios J J 2018 *Beilstein J. Nanotechnol.* **9** 1015
[11] Kresse G and Furthmüller J 1996 *Computational Materials Science* **6** 15–50
[12] Blaha P, Schwarz K, Madsen G, Kvasnicka D and Luitz J 2001 *Wien2k: An augmented plane wave+ local orbitals program for calculating crystal properties* (Karlheinz Schwarz, Techn. Universität Wien, Austria) ISBN 3-9501031-1-2
[13] Giannozzi P *et al.* 2009 *J. Phys.: Condens. Matter* **21** 395502
[14] Ozaki T 2003 *Phys. Rev. B* **67**(15) 155108
[15] Ozaki T and Kino H 2004 *Phys. Rev. B* **69**(19) 195113
[16] Ozaki T and Kino H 2005 *Phys. Rev. B* **72**(4) 045121
[17] Ozaki T *et al.* 2017 OpenMX (Open source package for Material eXplorer) ver. 3.8 URL http://www.openmx-square.org/
[18] Dovesi R *et al.* 2014 *Int. J. Quantum Chem.* **114** 1287
[19] Frisch M J *et al.* Computer code GAUSSIAN09, Revision C.01, Gaussian, Inc. Wallingford, CT, 2009
[20] Barreteau C, Spanjaard D and Desjonquères M C 2016 *Comptes Rendus Physique* **17** 406
[21] Lejaeghere K *et al.* 2016 *Science* **351**
[22] Ozaki T 2019 Delta gauge of OpenMX with the database (2019) URL https://t-ozaki.issp.u-tokyo.ac.jp/vps_pao2019/Delta_Factor/index.html
[23] Laun J and Bredow T 2021 *Journal of Computational Chemistry* **42** 1064–1072
[24] Sabater C, Dednam W, Calvo M R, Fernández M A, Untiedt C and Caturla M J 2018 *Phys. Rev. B* **97** 075418
[25] Calvo M R, Sabater C, Dednam W, Lombardi E B, Caturla M J and Untiedt C 2018 *Phys. Rev. Lett.* **120**(7) 076802
[26] Ruiz E, Llunell M and Alemany P 2003 *Journal of Solid State Chemistry* **176** 400–411
[27] Palacios J J, Pérez-Jiménez A J, Louis E and Vergés J A 2001 *Phys. Rev. B* **64**(11) 115411
[28] Palacios J J, Pérez-Jiménez A J, Louis E, SanFabián E and Vergés J A 2002 *Phys. Rev. B* **66**(3) 035322
[29] Louis E, Vergés J A, Palacios J J, Pérez-Jiménez A J and SanFabián E 2003 *Phys. Rev. B* **67**(15) 155321
[30] Palacios J J *et al.* Computer code ANT.Gaussian, with SOC corrections Available from https://github.com/juanjosepalacios/ANT.Gaussian
[31] Jacob D and Palacios J J 2011 *The Journal of Chemical Physics* **134** 044118
[32] Zotti L A and Pérez R 2017 *Phys. Rev. B* **95**(12) 125438
[33] Ozaki T, Nishio K and Kino H 2010 *Phys. Rev. B* **81** 035116 ISSN 1098-0121
[34] Laun J, Vilela Oliveira D and Bredow T 2018 *Journal of Computational Chemistry* **39** 1285–1290
[35] Jungwirth T, Wunderlich J and Olejník K 2012 *Nature Materials* **11** 382–390